

# Simple and Rapid Quantification of Thrombocytes in Zebrafish Larvae

Michael C. Hwang and Jordan A. Shavit

## Abstract

Platelets are a critical component of hemostasis, with disorders of number or function resulting in coagulation disturbances. Insights into these processes have primarily been realized through studies using mammalian models or tissues. Increasingly, zebrafish embryos and larvae have been used to study the protein and cellular components of hemostasis and thrombosis, including the thrombocyte, a nucleated platelet analog. However, investigations of thrombocytes have been somewhat limited due to lack of a robust and simple methodology for quantitation, an important component of platelet studies in mammals. Using video capture, we have devised an assay that produces a rapid, reproducible, and precise measurement of thrombocyte number in zebrafish larvae by counting fluorescently tagged cells. Averaging 1000 frames, we were able to subtract background fluorescence, thus limiting assessment to circulating thrombocytes. This method facilitated rapid assessment of relative thrombocyte counts in a population of 372 zebrafish larvae by a single operator in less than 3 days. This technique requires basic microscopy equipment and rudimentary programming, lends itself to high throughput analysis, and will enhance future studies of thrombopoiesis in the zebrafish.

## Introduction

**P**LATELETS PLAY AN INTEGRAL ROLE in maintaining hemostasis. In response to vascular injury, platelets interact with von Willebrand factor (VWF) to initiate adhesive reactions, resulting in formation of the “platelet plug.” These events, collectively known as primary hemostasis, serve as the first line of defense in restoring the integrity of the vascular wall.<sup>1</sup> Defects in platelet number or function often result in primary hemostatic disorders or thrombotic events such as myocardial infarction and stroke.<sup>2,3</sup>

A significant body of research has been dedicated to the identification of proteins that regulate platelet number and function with the goal of developing therapies for affected individuals. Through genome-wide association and proteomic studies, a number of genes have been recognized to play a role in platelet activity.<sup>4,5</sup> Efforts to identify and study these genes have utilized various animal models, including zebrafish. The zebrafish, *Danio rerio*, has risen to become a popular choice to analyze gene function during development and model human disease *in vivo*.<sup>6</sup> Small in size with a high fecundity, zebrafish is a well-characterized vertebrate with a fully sequenced genome and conservation of nearly all coagulation factors.<sup>7,8</sup> Early larvae and embryos are transparent, permitting observation of circulation through light microscopy.

Multiple studies have demonstrated functional conservation of zebrafish thrombocytes with mammalian platelets, and fish have aided in the unraveling of several human genetic platelet disorders (reviewed in Refs.<sup>3,8,9</sup>). Unlike mammals, zebrafish thrombocytes are nucleated, but they share structural and functional features with platelets. For example, both contain an open canalicular system and form pseudopodia on activation.<sup>10</sup> Orthologs for many mammalian platelet proteins, such as VWF and CD41, are also present.<sup>11–13</sup>

Transgenic technology has allowed the development of zebrafish with fluorescently tagged cell populations, including a thrombocyte line. This strain expresses green fluorescent protein (GFP) under regulation of the *cd41* promoter, and it has been used for multiple studies that have led to novel insights into platelet function.<sup>3,8,9</sup> Quantitative analysis of thrombocytes has relied on *in vivo* or *ex vivo* flow cytometry<sup>14,15</sup> or peripheral blood smears.<sup>10</sup> However, these methods usually require euthanasia for blood collection and/or time-consuming and expensive analyses.

Previously, a simple and high-throughput method for relative quantification of fluorescently tagged leukocytes in zebrafish embryos using a linearly proportional parameter termed “leukocyte units” has been described.<sup>16</sup> In addition, video frame subtraction has been utilized to analyze circulatory system characteristics during zebrafish development.<sup>17</sup> Here, we present adaption of these techniques to develop a

similar comparative measure of circulating thrombocytes in zebrafish larvae, using video to eliminate stationary cells and background fluorescence. We show that this analysis requires minimal effort, is reproducible, and provides a practical method for rapid quantification of relative thrombocyte counts (“thrombocyte units” [TU]) in zebrafish larvae.

## Materials and Methods

### Animals

Zebrafish were raised in accordance with animal care guidelines<sup>18</sup> approved by the University of Michigan Animal Care and Use Committee. All experiments were performed using the *cd41-egfp* transgenic line.<sup>14</sup> Harvested embryos were incubated in methylene blue containing system water at 28°C with 0.003% 1-phenyl-2-thiourea (PTU; Sigma-Aldrich, St. Louis, MO) at a density of 50–100 per 100 mm dish. Petri dishes were stored in a 28°C incubator until analysis at 6 days postfertilization (dpf).

### Mounting of larvae for imaging

At 6 dpf, zebrafish larvae were anesthetized using tricaine (0.16 mg/mL; Western Chemical, Inc., Ferndale, WA) followed by immersion in 0.7% low-melting point agarose. Up to three larvae were loaded in 100 mm long, 1.5–1.8 mm outer diameter range glass capillaries (Pyrex). Each larva was separated by an air bubble to prevent mixing and facilitate unloading. Loaded capillaries were placed onto modeling clay for stabilization in a plastic tray, followed by submersion in water to minimize refraction.

### Imaging system

A Leica MZ16FA microscope (Leica, Wetzlar, Germany) was equipped with a Canon 60D digital single lens reflex

(DSLR) camera using an AmScope microscope adapter (United Scopes, LLC, Irvine, CA), which was mounted on the viewport. Magic Lantern ([www.magiclantern.fm](http://www.magiclantern.fm)), a free firmware add-on for Canon EOS DSLR cameras, was installed, allowing adjustment of parameters such as sensitivity (ISO) and frame-rate. An external remote was attached to the camera to reduce vibratory movements associated with activation of the shutter for recording.

### Imaging procedure

Larvae were visualized at 85× magnification through a GFP2 long-pass filter (Leica) and identical regions were framed in each individual, from the anterior tip of the larvae to the yolk sac extension, all of which were within the same focal plane (Fig. 1A). With the DSLR camera set to video mode, “ISO” was set to 6400 and “FPS override” was enabled. “Desired FPS” was set to 20 with a “Shutter range” of 1/20–1/59 through the Magic Lantern context menu. The “Movie REC key” was modified from default to HalfShutter to allow the external remote to control recording. Each movie was recorded for 1 min at 1920×1080 resolution. Videos were stored on an internal SD card, and no computer was required for image capture. A raw sample frame is shown in Figure 1B.

### Image processing

Subsequent video processing was performed using Adobe AfterEffects (Adobe, San Jose, CA) and ImageJ<sup>19</sup> software. Each video was processed initially to reduce noise from the low-light conditions using Adobe AfterEffects and the NeatVideo plugin ([www.neatvideo.com](http://www.neatvideo.com)) on a Macintosh computer (both are also available for Windows). The NeatVideo reduce noise feature is based on the principle of image denoising. Noise is a random variation of brightness or color that manifests as a grain-like appearance, usually in areas of

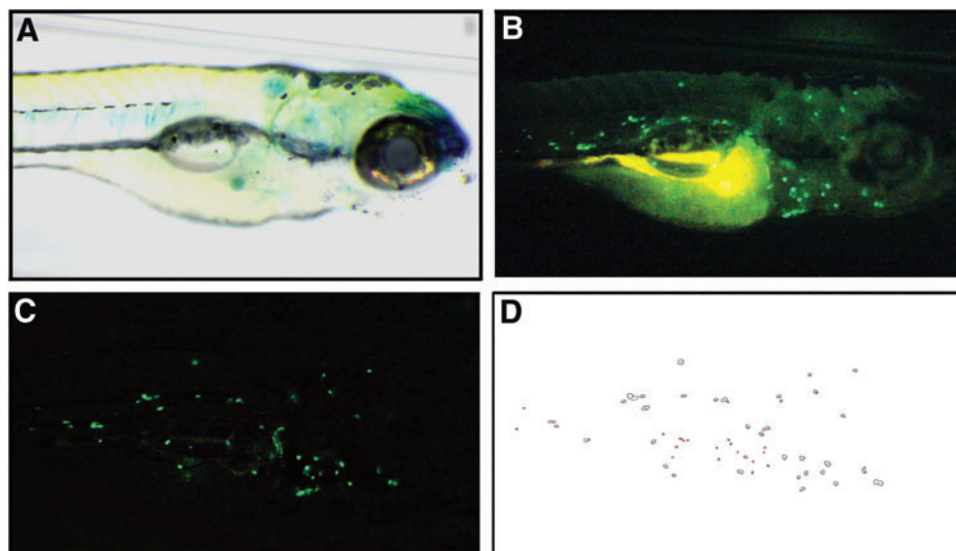


**FIG. 1.** Sample work flow of image processing of a single frame acquired from a *cd41-egfp* transgenic larva. Green fluorescence indicates specific *egfp* expression in thrombocytes or autofluorescence in the yolk sac. (A) Brightfield image demonstrating the orientation of 6 days postfertilization (dpf) larvae and positioning from the anterior tip of the larvae to the beginning of the yolk sac extension. (B) Raw fluorescence image before processing shows circulating and nonmobile thrombocytes, as well as background and autofluorescence. (C) Frame postprocessing showing circulating thrombocytes. (D) ImageJ “analyze particle” visual output of thrombocyte units (TU). Color images available online at [www.liebertpub.com/zeb](http://www.liebertpub.com/zeb)

low light where only a small amount of information can be derived. Each camera produces its own unique image noise.<sup>20</sup> The goal of image denoising ultimately aims at preserving image features such as texture while eliminating noise.<sup>20</sup> NeatVideo assists in semi-automating this process by allowing the user to establish a baseline level of noise by indicating a “smooth image” region in an image frame. This region becomes the featureless area in which to profile noise and serves as the threshold that could be applied to the remainder of the image frame. The parameters for the “Reduce Noise” effect were a temporal filter radius of 5, a temporal filter threshold of 100%, and a device noise profile taken from the top right corner of the video as reference. A script was created to automate these steps for high-throughput analysis. Once the “Reduce Noise” effect was applied, all of the compositions were selected and added to the render queue to allow for processing (Composition → Add to Render Queue). Each video was processed and saved in a lossless (uncompressed) format for subsequent processing in ImageJ.

After noise reduction, the resulting video file was imported and converted into a virtual stack in ImageJ. From there, an average frame was produced from the stack of 1000 frames using the “Z Project...” command with “Average Intensity” selected. The average frame that was produced was subtracted to each frame in the virtual stack using the “Subtract create stack” command, which resulted in a video of only circulating thrombocytes (Fig. 1C). From there, a threshold (0.5) was applied and colors were converted into binary colors using “Invert” in preparation for thrombocyte counting. “Analyze Particles...” was used with the parameters of “size = 12–6000” and “circularity = 0.40–1.00” for thrombocyte counting (Fig. 1D). The resulting thrombocyte numbers (termed TU) were collected and exported as a text document for data processing and analysis (Microsoft Excel and GraphPad). These steps were also automated within ImageJ through a custom macro for high-throughput analysis.

#### Manual thrombocyte counts

Thrombocytes were counted manually in every 50th frame after background subtraction. This was performed till the 500th frame, and these manual counts were plotted against the corresponding automated count generated from that same image in the “Analyze Particles” feature of ImageJ.

## Results

#### Visualization of circulating thrombocytes through video-assisted background subtraction

During embryonic and larval development, both circulating and nonmobile GFP<sup>+</sup> cells are visible, and data suggest that the latter represent hematopoietic progenitors.<sup>14</sup> To quantify the thrombocyte population, we developed a protocol to rapidly identify just the circulating GFP<sup>+</sup> cells. We were able to fine tune video recording parameters such as sensitivity and frame-rate using a camera firmware add-on, which was critical in viewing the fluorescently labeled circulating thrombocytes in low light conditions. The principle behind image subtraction, which enabled removal of background, is the separation of static and dynamic pixels; these are areas where no movement is detected.<sup>17</sup> Each pixel has an assigned grayscale value in each frame. A composite image

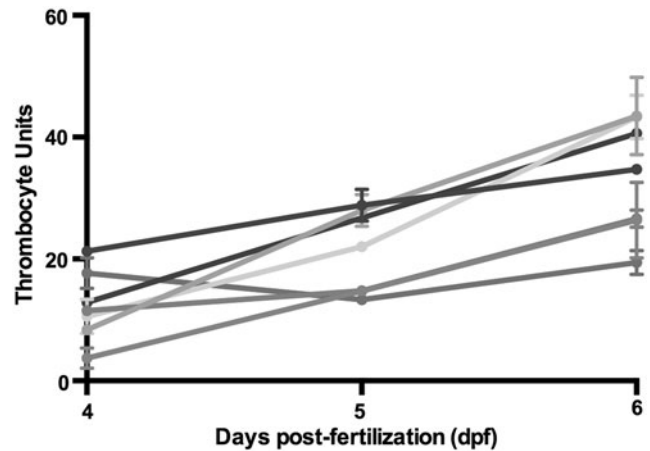


**FIG. 2.** Thrombocyte units (TU) measured in individual larvae from 4 to 6 dpf. Each line represents an individual larva. Each measurement represents the average TU of 1000 frames at that point in time, and error bars represent the standard deviation of that measurement.

was created from all frames in a reference video, and in this image each pixel was the average intensity from all the frames. The composite served as a background image, which was used to determine which pixels in each individual frame were dynamic or static. This was accomplished by subtracting the composite image from each frame individually, and it resulted in a clear separation from the static and dynamic pixels, enabling discernment of circulating and noncirculating thrombocytes (Fig. 1B vs. C). For each video, quantification of circulating thrombocytes was performed for each frame and then averaged across all frames. This final number was termed thrombocyte units (TU).

#### Circulating thrombocyte counts are accurate and reproducible

During embryogenesis in *cd41-egfp* zebrafish, the population of GFP<sup>+</sup> circulating thrombocytes expands, after first

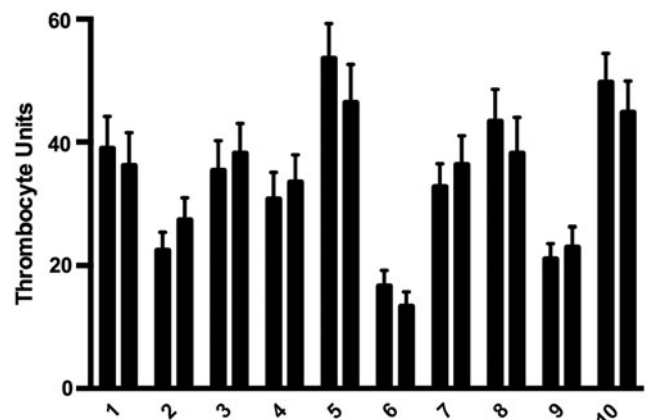


**FIG. 3.** Repeat TU measurements on individual larvae. Duplicate measurements were taken from 10 individual 6 dpf larvae, ~30 min apart. Each repeat data collection was performed after a capillary was removed and remounted. Each single measurement represents the average TU of 1000 frames at that point in time, and error bars represent the standard deviation of that measurement.

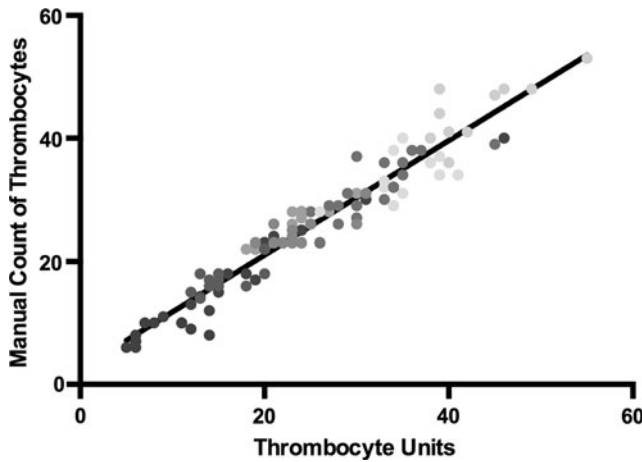


**FIG. 4.** Comparison of manual counts versus TU. Manual counts were performed on 10 frames each of 10 individuals after processing and background subtraction. The results were plotted against the TU from the same frame. Linear regression was performed, yielding an R-square of 0.93.

becoming visible at 3–4 dpf.<sup>14</sup> We initially determined whether thrombocytes increase in quantity during development by examining seven zebrafish larvae at 4, 5, and 6 dpf (Fig. 2). Except for a single outlier, larvae demonstrated an increasing number of TU each day, and we concluded that the optimum time point for imaging was 6 dpf.

The reproducibility of the video analysis was assessed by performing repeat measurements on individual larvae. Capillaries containing larvae were mounted, imaged, removed, and remounted 30 min later for repeat imaging. With each mounting, we were able to achieve quick and precise orientation of larvae by simple rotation of the capillary, and there were minimal changes between repeat measurements (Fig. 3).

Manual counting of thrombocytes was performed to confirm the accuracy of the automated calculations. Ten fish larvae were video recorded, processed, and thrombocytes

were counted manually in 10 nonconsecutive frames from each individual. Each manual count was compared with the automated count for that frame (Fig. 4). Linear regression demonstrated a high degree of correlation with an R-square of 0.93.

#### *Population distribution of thrombocytes in larvae*

To assess the distribution of TU across a large population of *cd41-egfp* larvae, 372 individuals were analyzed at 6 dpf. The mean count was  $25 \pm 10$  TU per individual larva, and 87.6% of the population were within a four-fold range (10–40 TU/larva, Figure 5).

#### **Discussion**

One of the distinct advantages of the zebrafish model is high-throughput genetic and small-molecule screens in embryos and larvae. Such experiments have not yet been performed to study thrombopoiesis, and one reason may have been the lack of a high-throughput method for quantification of thrombocytes. Using a transgenic line with fluorescently tagged thrombocytes, we have developed a method that is modeled after a technique used to count fluorescently tagged leukocytes in embryos.<sup>16</sup> These computational methods are simple and have the potential for high-throughput quantification of large numbers of individuals. One potential drawback of the approach used for leukocytes is reduced precision due to quantification of a single image. This method could be a shortcoming for thrombocytes, in particular, since it counts all GFP<sup>+</sup> cells, and the *cd41-egfp* transgene is known to mark stationary hematopoietic precursors as well as circulating thrombocytes.<sup>14</sup> We have demonstrated that the use of video can overcome this limitation. The analysis of 1000 images over a defined period prevents a poor quality image from affecting the overall TU calculation, reduces scatter, and enhances precision. This was confirmed by repeat testing on individuals as well as by a comparison of automated to manual quantification on multiple individual images.

Through quantitation of a string of sequential images, we were able to average the results and subtract background fluorescence. This background included autofluorescence as well as stationary cells *in situ*, with the remaining signal consisting of circulating, mature thrombocytes. Our data prove that this methodology is both reliable and precise, requires minimal effort, and can be easily adapted to basic microscopic equipment with fluorescence capabilities. This inexpensive setup only requires a DSLR that can be mounted to a range of microscope viewports or eyepieces with commercially available adapters. Video processing and analysis is automated through simple scripts (available on request), allowing substantial numbers of individuals to be processed in parallel.

We evaluated relative thrombocyte counts in a large population of individuals at 6 dpf. Video recording and analysis of nearly 400 *cd41-egfp* larvae was rapidly performed in a few days by a single operator, which is high throughput compared with currently available methods. The TU population distribution, with almost 90% of individuals spread over a four-fold range, bears resemblance to platelet count variation in the normal human population.<sup>2</sup> One limitation to this method is that it is a relative measure of thrombocytes, and not necessarily the actual total count in an individual.

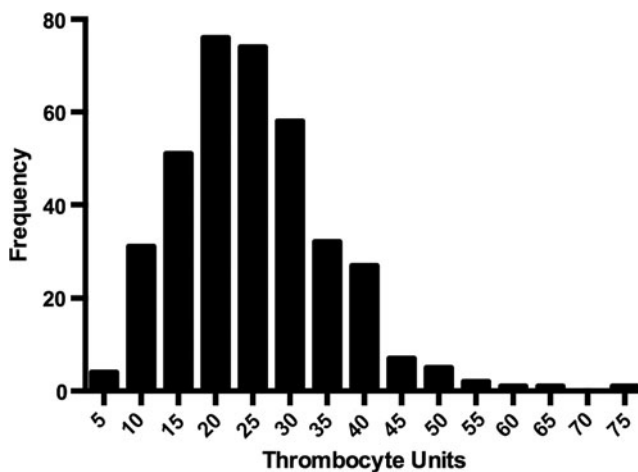


**FIG. 5.** Population distribution of TU in 6 dpf larvae. Histogram of TU from 372 zebrafish larvae measured at 6 dpf indicates that 87.6% varied over a four-fold range (10–40 TU/larva). Each label on the x-axis indicates a bin with a range of 5 TU, with the number representing the maximum for that bin, for example, 5 = 1–5 TU, 10 = 6–10 TU, etc.

Although studies of pathologic states have yet to be performed, we speculate that this technique can be utilized to determine deviation of mutant or treated groups from controls, enabling genetic and small-molecule screens. In conclusion, we have developed a rapid and simple nonlethal method for relative quantification of thrombocytes in zebrafish larvae *in vivo*. We expect that this will facilitate modeling and high-throughput studies of thrombocytopenia or thrombocytosis in zebrafish.

### Acknowledgments

The authors thank Tim Baranowski for helpful suggestions, Angela Weyand for a critical reading of this article, and Zachary Norris for technical support. The authors also thank Bob Handin for providing the *cd41-egfp* transgenic line. This work was supported by an American Society of Hematology HONORS Award (M.C.H.), Pfizer ASPIRE Award (J.A.S.), and NICHD HD028820 (J.A.S.). J.A.S. is the Diane and Larry Johnson Family Scholar of Pediatrics and Communicable Diseases.

### Disclosure Statement

No competing financial interests exist.

### References

1. Newman PJ, Newman DK: Platelets and the vessel wall. In: Nathan and Oski's Hematology of Infancy and Childhood. Orkin SH, Nathan DG, Ginsburg D, Look AT, Fisher DE, and Lux SE (eds), pp. 1379–1398, 7th ed., Saunders Elsevier, Philadelphia, PA, 2009.
2. Lambert MP, Poncz M. Inherited platelet disorders. In: Nathan and Oski's Hematology of Infancy and Childhood. Orkin SH, Nathan DG, Ginsburg D, Look AT, Fisher DE, Lux SE (eds), pp. 1463–1486, 7th ed., Saunders Elsevier, Philadelphia, PA, 2009.
3. Thijs T, Deckmyn H, Broos K. Model systems of genetically modified platelets. *Blood* 2012;119:1634–1642.
4. Bunimov N, Fuller N, Hayward CP. Genetic loci associated with platelet traits and platelet disorders. *Semin Thromb Hemost* 2013;39:291–305.
5. Burkhart JM, Gambaryan S, Watson SP, Jurk K, Walter U, Sickmann A, *et al.* What can proteomics tell us about platelets? *Circ Res* 2014;114:1204–1219.
6. Santoriello C, Zon LI. Hooked! modeling human disease in zebrafish. *J Clin Invest* 2012;122:2337–2343.
7. Howe K, Clark MD, Torroja CF, Torrance J, Berthelot C, Muffato M, *et al.* The zebrafish reference genome sequence and its relationship to the human genome. *Nature* 2013;496:498–503.
8. Weyand AC, Shavit JA. Zebrafish as a model system for the study of hemostasis and thrombosis. *Curr Opin Hematol* 2014;21:418–422.
9. Khandekar G, Kim S, Jagadeeswaran P. Zebrafish thrombocytes: functions and origins. *Adv Hematol* 2012;2012:857058.
10. Jagadeeswaran P, Sheehan JP, Craig FE, Troyer D. Identification and characterization of zebrafish thrombocytes. *Br J Haematol* 1999;107:731–738.
11. Kim S, Radhakrishnan UP, Rajpurohit SK, Kulkarni V, Jagadeeswaran P. Vivo-Morpholino knockdown of alphaIIb: a novel approach to inhibit thrombocyte function in adult zebrafish. *Blood Cells Mol Dis* 2010;44:169–174.
12. Carrillo M, Kim S, Rajpurohit SK, Kulkarni V, Jagadeeswaran P. Zebrafish von Willebrand factor. *Blood Cells Mol Dis* 2010;45:326–333.
13. Ghosh A, Vo A, Twiss BK, Kretz CA, Jozwiak MA, Montgomery RR, *et al.* Characterization of zebrafish von Willebrand factor reveals conservation of domain structure, multimerization, and intracellular storage. *Adv Hematol* 2012;2012:214209.
14. Lin HF, Traver D, Zhu H, Dooley K, Paw BH, Zon LI, *et al.* Analysis of thrombocyte development in CD41-GFP transgenic zebrafish. *Blood* 2005;106:3803–3810.
15. Zhang L, Alt C, Li P, White RM, Zon LI, Wei X, *et al.* An optical platform for cell tracking in adult zebrafish. *Cytometry A* 2012;81:176–182.
16. Ellett F, Lieschke GJ. Computational quantification of fluorescent leukocyte numbers in zebrafish embryos. *Methods Enzymol* 2012;506:425–435.
17. Schwerte T, Pelster B. Digital motion analysis as a tool for analysing the shape and performance of the circulatory system in transparent animals. *J Exp Biol* 2000;203:1659–1669.
18. Westerfield M: The Zebrafish Book. A Guide for the Laboratory Use of Zebrafish (*Danio rerio*). 4th ed. University of Oregon Press, Eugene, OR, 2000.
19. Schneider CA, Rasband WS, Eliceiri KW. NIH Image to ImageJ: 25 years of image analysis. *Nat Methods* 2012;9:671–675.
20. Ce L, Szeliski R, Sing Bing K, Zitnick CL, Freeman WT. Automatic estimation and removal of noise from a single image. *IEEE Trans Pattern Anal Mach Intell* 2008;30:299–314.

Address correspondence to:  
Jordan A. Shavit, MD, PhD

Department of Pediatrics and Communicable Diseases  
University of Michigan  
Room 8301 Medical Science Research Building III  
1150 West Medical Center Drive  
Ann Arbor, MI 48109-5646  
E-mail: jshavit@umich.edu